

Article

Investigating the Potential of a Transparent Xanthan Polymer for Enhanced Oil Recovery: A Comprehensive Study on Properties and Application Efficacy

Gerd Hublik ¹, Riyaz Kharrat ^{2,*}, Ali Mirzaalian Dastjerdi ² and Holger Ott ²¹ Jungbunzlauer Austria AG, 2064 Wulzeshofen, Austria; gerd.hublik@jungbunzlauer.com² Department Geoenergy, Montanuniversität Leoben, 8700 Leoben, Austria; ali.mirzaalian@gmail.com (A.M.D.); holger.ott@unileoben.ac.at (H.O.)

* Correspondence: riyaz.kharrat@unileoben.ac.at

Abstract: This study delves into the properties and behavior of xanthan TNCS-ST, a specialized variant designed for enhanced oil recovery (EOR) purposes. A notable aspect of this polymer is its transparency and capability to dissolve in high salt concentrations, notably up to 18% total dissolved solids. Various laboratory methods are employed to assess the polymer's distinctive traits, including transparency, salt tolerance, and high pyruvylation. These methods encompass preparing xanthan solutions, conducting filtration tests, assessing energy consumption, and measuring rheological properties. The findings highlight the influence of salt concentration on xanthan's filterability, indicating increased energy requirements for dissolution with higher salt and xanthan concentrations. Additionally, this study observes temperature-dependent viscosity behavior in different solutions and evaluates the shear stability of xanthan. A significant and novel characteristic of TNCS-ST is its high salt tolerance, enabling complete dissolution at elevated salt concentrations, thus facilitating the filterability of the xanthan solution with sufficient time and energy input. Core flooding experiments investigate fluid dynamics within porous rock formations, particularly sandstone and carbonate rocks, while varying salinity. The results underscore the substantial potential of the new xanthan polymer, demonstrating its ability to enhance oil recovery in sandstone and carbonate rock formations significantly. Remarkably, the study achieves a noteworthy 67% incremental recovery in carbonate rock under the high salinity level tested, suggesting promising prospects for advancing enhanced oil recovery applications.

Keywords: xanthan; filtration; rheological properties; salt tolerance; enhanced oil recovery (EOR)

Citation: Hublik, G.; Kharrat, R.; Dastjerdi, A.M.; Ott, H. Investigating the Potential of a Transparent Xanthan Polymer for Enhanced Oil Recovery: A Comprehensive Study on Properties and Application Efficacy. *Energies* **2024**, *17*, 1266. <https://doi.org/10.3390/en17051266>

Academic Editor: Dameng Liu

Received: 31 January 2024

Revised: 28 February 2024

Accepted: 3 March 2024

Published: 6 March 2024



Copyright: © 2024 by the authors. Licensee MDPI, Basel, Switzerland. This article is an open access article distributed under the terms and conditions of the Creative Commons Attribution (CC BY) license (<https://creativecommons.org/licenses/by/4.0/>).

1. Introduction

Xanthan, a polysaccharide produced by the bacterium *Xanthomonas campestris*, is a viscosifier and stabilizer in various applications, including food, feed, and personal care products. However, its largest application is in the oil industry. Xanthan finds utility in drilling mud, workover, and completion fluids and is a crucial component for mobility control in polymer flooding and enhancing oil recovery [1–6].

Enhanced oil recovery seeks to extract additional oil from reservoirs when secondary production methods, typically waterflooding, become economically unviable. The selection of an appropriate recovery method hinges on the physical and chemical characteristics of the oil reservoir, such as temperature, oil viscosity, formation type, and permeability [7]. Polymer flooding has emerged as a standard approach for tertiary oil recovery among the available methods [8]. Various EOR projects employing polymers in the field have been documented by researchers [9], with 51 out of 72 projects deemed successful or promising, while only 6 were considered discouraging. Polymers are introduced into aqueous solutions to increase viscosity and reduce mobility, thereby enhancing the efficiency of waterflooding [10].

A study assessed the impact of temperature and monovalent salts, specifically sodium chloride (NaCl), at various temperatures on the rheological behavior of xanthan gum for EOR applications [11]. The findings revealed that fluctuations in temperature notably influenced viscosity, while monovalent salts mitigated adverse thermal effects. Surprisingly, an unforeseen increase in solution viscosity was observed with higher monovalent salt concentrations, shedding light on xanthan gum's potential suitability for EOR amidst challenging reservoir conditions.

In the industry, two polymers are utilized: polyacrylamides, produced through chemical processes, and polysaccharides, produced via microorganism-based fermentation. Although polyacrylamides and their derivatives remain the most prevalent choice for EOR, they are susceptible to high shear forces and do not tolerate elevated salt concentrations, especially calcium or magnesium levels [4,12,13]. Furthermore, hydrolyzed polyacrylamide (HPAM), the most commonly used derivative in polymer flooding, fails to pass the standard OECD 306 biodegradation test. Consequently, HPAM is subject to a level-4 substitution warning on the U.K. continental shelf and is classified as a red chemical in Norway [14,15].

In a review of seventy-two polymer projects, only four field trials involving biopolymers employed xanthan gum [9]. Three trials were considered successful or promising, while one was deemed too early to assess. A successful pilot test using xanthan in the Shengli Oil Field in China was also documented [16]. Currently, field trials for polymers typically undergo a rigorous evaluation process in the laboratory to ensure that the material meets specific criteria and is suitable for real-world applications [4,17–20]. The specific criteria can vary depending on the intended use of the polymer, but here are some common factors that are typically assessed:

1. **Filterability:** to ensure the polymer solution is free of cell debris and aggregates that could lead to formation plugging, injectivity reduction, permeability decrease, or even formation fracturing, a filter test is recommended by the American Petroleum Institute and several authors [5,6,12,21,22].
2. **Viscosity at reservoir conditions and long-term stability:** Since polymer flooding extends for over 6 months, it must retain its viscosity under reservoir conditions. Under ideal conditions (no dissolved oxygen, pH 7 to 8, and moderate-to-high salinities), xanthan solutions may exhibit half-lives of up to five years at temperatures between 75 and 80 °C [23]. Xanthan's stability in seawater for 800 days at 80 °C and even better stability at 90 °C in a 50 g/L NaCl solution than 1 g/L NaCl have been confirmed [24,25]. Furthermore, it was found that xanthan remained stable for more than three years in a successful polymer pilot test conducted in the Eddesse-Nord EOR project in Germany [26].
3. **Shear stability:** In both the injection process and the formation, mechanical stress can lead to polymer molecule degradation and viscosity loss if shear forces are excessively high [10]. Xanthan exhibits remarkable shear stability, withstanding shear rates as high as 870,000/s [13].
4. **Compatibility with high salt concentrations:** Oil reservoirs often vary in salinity, ranging from 0.3% to 22% salt concentrations [9]. Using appropriate equipment featuring high shear rates, xanthan can dissolve in saturated mono- and divalent brines [27].
5. **Adsorption behavior:** As polymers flow through porous rock, some degree of polymer retention occurs due to physicochemical adsorption, mechanical entrapment in pores, and hydrodynamic retention [28]. Xanthan adsorption has been shown to depend on soil type and polymer concentration, typically remaining below 0.3 mg/g for all tested soil types at a xanthan concentration of 1 g/L [20]. In a polymer pilot test, adsorption was reported to range from 30 to 40 µg xanthan per gram of soil [26].

Compliance with these laboratory criteria is crucial for preparing the polymer for field trials and ensuring its dependable performance in practical scenarios. Depending on the unique demands of the application, additional assessment parameters and testing protocols may be necessary. Engaging domain experts is essential, and it is crucial to

consider any industry-specific standards or guidelines relevant to the specific polymer application in question.

While xanthan gum presents numerous advantages for EOR applications, including its non-Newtonian rheological behavior, high viscosity, thermal stability, relative insensitivity to salinity and temperature, and environmentally friendly characteristics, it also has limitations. One notable deficiency is its compatibility with specific reservoir conditions, particularly in highly saline and high-temperature environments. Moreover, its performance can be compromised by monovalent and divalent cations, reducing viscosity and effectiveness in mobility control. Modifying xanthan and its preparation methods can significantly influence its application in EOR. An experimental study conducted in 2021 presented a modification of the chemical structure of xanthan gum with acrylic acid through a chemical process to scrutinize the rheological properties and EOR potential [29]. The oil recovered from the sandstone cores reflected the improvement in the viscosity of xanthan gum after its modification.

Further research is necessary to delve deeper into the method of preparing modified xanthan gum for EOR applications. Specifically, studies should focus on refining the chemical process of modifying xanthan gum to optimize the modified polymer's rheological properties and EOR potential. Additionally, investigations into novel preparation methods, such as alternative synthesis routes or post-modification techniques, could provide valuable insights into improving the compatibility and performance of modified xanthan gum in challenging reservoir environments.

This study aims to elucidate key findings regarding a novel xanthan material, specifically its suitability for polymer flooding. The research encompasses crucial energy data necessary for dissolving this specific xanthan variant to achieve an acceptable filtration ratio. Furthermore, the study provides insights into flow curves, temperature-dependent viscosity changes, and the stability of this biopolymer under high-shear conditions across various brine solutions while assessing its impact on oil recovery.

2. Methodology

The methodology of this study entailed a systematic approach to preparing and analyzing xanthan solutions for EOR investigations. Initially, a screening process was conducted to identify the xanthan type exhibiting the highest viscosity. Preparing the xanthan solutions involved dissolving salts, adjusting the pH, and mixing using a laboratory mixer. Filtration techniques were then applied to eliminate insoluble particles, while energy consumption during mixing was quantified. Rheological measurements offered insights into solution flow behavior and viscosity. Molecular analysis methods, such as FT-IR analysis and hydrolysis, were employed to examine the structure and composition of xanthan. Finally, core flooding experiments were conducted to simulate fluid behavior in porous rock formations, assessing the efficacy of xanthan in enhancing oil recovery by monitoring various parameters. This comprehensive methodology provides a structured approach to investigate the performance of xanthan in EOR applications.

2.1. Raw Material

In this study, we employed a specific xanthan variant known as xanthan TNCS-ST, sourced from Jungbunzlauer, Wulzeshofen, Austria, tailored for EOR applications. The TNCS-ST xanthan consists of the typical xanthan pentasaccharide unit, as shown in Figure 1. Sodium ions are bound to the carboxylic groups of pyruvate and glucuronic acid [30,31]. The unique feature of the xanthan TNCS polymer lies in its transparency and solubility in high salt concentrations; particularly notable is its compatibility with solutions containing up to 18% total dissolved solids. This xanthan material is characterized by its cell-free, transparent nature and impressive salt tolerance. It boasts high pyruvylation (~6%) and acetylation (~4.5%). When utilizing fermentation broth for the filtration tests, the broth underwent enzymatic treatment to degrade bacterial cells and was subsequently heat-treated at 95 °C for 20 min. The salts used in brine preparation were of analytical-grade quality.

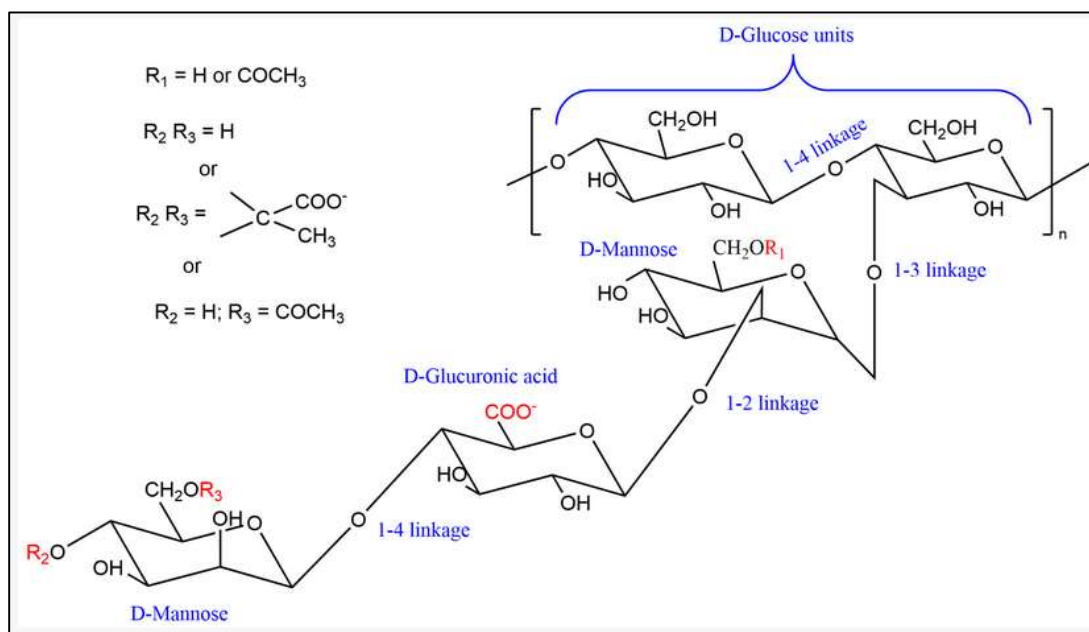


Figure 1. Structure of the xanthan TNCS-ST polymer [31].

2.2. Preparation of Xanthan Solution

The process involved dissolving salts in distilled water, with pH adjustments achieved using 0.1 M NaOH or HCl. Subsequently, all brine solutions underwent filtration through a 1.2 μm Isopore membrane filter from Merckmillipore, Darmstadt, Germany, to eliminate insoluble particles. Unless specified otherwise, the dissolution process entailed mixing 1 g of xanthan with 1 L of distilled water or brine. This mixing was performed using an L5T laboratory mixer equipped with a high-shear screen work head from Silverson Machines Ltd., Chesham, UK, which generated a shear rate of 42,935/s at 8000 rpm (data provided by Silverson Machines). The mixer's speed was adjusted to 1 Ampere, approximately 8000 rpm, depending on the xanthan concentration. Following each one-minute incremental mixing step, the mixture underwent de-foaming and de-aeration before filtration. To prevent overheating due to the mixer's energy input, the containers holding the xanthan solution were placed in a water bath set to 27 $^{\circ}\text{C}$. In cases where xanthan was dissolved at 60 $^{\circ}\text{C}$, the solutions were subsequently cooled in a water bath to 30 $^{\circ}\text{C}$ before filtration. Table 1 provides the composition details of the brines, with the formation water prepared following the method outlined in a previous study [32].

Table 1. Brine composition.

Composition	Sea Water (g/L)	High-Salinity Water (g/L)	Formation Water (g/L)
NaCl	30	85	132
KCl	0.7	0	0
CaCl ₂ ·2H ₂ O	1.53	13.2	56
MgCl ₂ ·6H ₂ O	11.1	10.7	22
Total dissolved solids (TDS)	37	100	185
pH value	8.2	6.0	6.0

2.3. Filtration

A 600 mL pressure vessel (XX1100000) with a 47 mm Swinnex filter holder from Millipore filtrated the xanthan solutions. All solutions were filtered through an Isopore Membrane Filter, 1.2 μm RTTP from Millipore with an overpressure of 0.1 MPa using compressed air. The elapsed time for every 100 mL of filtered solution was observed. The

filtration ratio (FR) was calculated according to the method of the American Petroleum Institute [6]:

$$FR = (t_{500\text{mL}} - t_{400\text{mL}}) / (t_{200\text{mL}} - t_{100\text{mL}})$$

2.4. Calculation of Energy

Our objective was to determine the electrical energy necessary to achieve a filtration ratio below 1.5. This was calculated by multiplying the electrical power: 230 Volts \times 1 Ampere = 230 Watts. Consequently, the electrical energy consumption equals 3.83 Watthours per liter (or 3.83 kWh/m³) per minute of mixing.

2.5. Rheological Measurement

The rheological characterization was conducted using an MCR 302 rheometer from Anton Paar, Graz, Austria. Flow curves were obtained using a cone–plate geometry with a 60 mm diameter and an angle of 0.5° (CP60-0.5/TI) from Anton Paar. Unless otherwise specified, flow curve measurements were performed at a temperature of 30 °C. Temperature-dependent viscosity data were acquired using a CC39 concentric cylinder from Anton Paar, maintaining a constant shear rate of 8/s.

2.6. Molecular Analysis of Xanthan

FT-IR analysis using a Bruker Alpha ATR device (Bruker Corporation, Billerica, MA, USA) was conducted to validate the xanthan structure qualitatively. For quantitative measurements, 1% xanthan underwent hydrolysis in 1 M H₂SO₄ for 4 h at 105 °C. Acetic acid and pyruvic acid were quantified utilizing assay kits from Megazyme Ltd., Wicklow, Ireland. Sodium and potassium quantifications were performed using inductively coupled plasma spectroscopy from Spectro Analytical Instruments (Spectro GmbH, Kleve, Germany). While FT-IR analysis is essential for identifying functional groups within xanthan, its ability to quantify subtle differences, such as the increased pyruvate content in TNCS-ST xanthan, may be limited. Despite the reported higher pyruvate content in TNCS-ST, this difference is not readily discernible in the spectra. Our observations suggest that while FT-IR is valuable for qualitatively distinguishing functional groups, its capacity for quantification may be somewhat restricted.

2.7. Core Flooding

Core flooding is a laboratory technique commonly used in EOR to simulate and study the behavior of fluids, typically reservoir core samples, in porous rock formations. This study conducted a flooding experiment using sandstone and carbonate rocks with different salinity and xanthan polymer concentrations. The core properties utilized in this study are outlined in Table 2.

Table 2. Core properties of sandstone and carbonate rocks.

Properties	Bentheimer Sandstone	Estailades Carbonate
Porosity, %	18.72	29.21
Permeability, mD	294.76	194.71
Core length (cm)	5.06	5.06
Core diameter (cm)	3.77	3.77

The process involves preparing a core sample saturated with brine and oil flooding to achieve residual water saturation. Water flooding displaces oil, and a polymer solution, prepared to increase water viscosity, is injected to aid in further oil displacement. The monitoring and evaluation of parameters assess the effectiveness of polymer flooding in enhancing oil recovery.

Displacement experiments were conducted using a core flood apparatus. The cores were initially saturated with a brine containing 60,000 ppm NaCl. An oil with 50 cp viscosity

was then injected. Oil injection continued until no further expulsion of brine occurred from the cores, thereby establishing irreducible water saturation. Subsequently, brine was introduced into the cores to replicate secondary oil recovery. The brine injection continued for two pore volumes. Two pore volumes of polymer solution of 1500 ppm were then injected into the core plugs in the tertiary oil recovery phase.

3. Results and Discussion

3.1. Viscosity of Various Xanthan Materials

An initial screening of various xanthan types was carried out to select the material with the highest viscosity in 4% NaCl solution. The molecular characteristics of the tested types are displayed in Table 3. Based on the flow curve results depicted in Figure 2, xanthan exhibiting high pyruvate content and featuring sodium attachment on the carboxylic groups was chosen for subsequent testing (sample 11). Consequently, all TNCS-ST xanthan samples utilized in this study were prepared following the protocol established for sample 11.

Table 3. Characteristics of tested xanthan samples used to select EOR material.

Sample ID	Acetate %	Pyruvate %	Na ⁺ %	K ⁺ %	Xanthan Material
1	7.5	2.8	2.6	0.3	Xanthan with reduced pyruvate
2	6.8	2.7	2.9	0.2	Xanthan with reduced pyruvate
3	0.5	6.8	3.1	0.3	Xanthan with low acetate
4	0.4	6.6	3.3	0.2	Xanthan with low acetate
5	7.4	0.2	2.2	0.2	Xanthan with low pyruvate
6	3.9	5.4	3.4	0.2	Xanthan from the original xanthan strain (NRRL B-1459)
7	4.6	6.3	3.4	0.4	Xanthan from the original xanthan strain (NRRL B-1459)
8	4.7	5.7	3.8	0.3	Xanthan with low viscosity
9	5.1	5.6	3.6	0.3	Xanthan with low viscosity
10	6.2	6.8	3.5	0.4	Xanthan with high pyruvate
11	5.6	5.9	3.2	0.4	Xanthan with high pyruvate
12	5.7	5.5	0.4	3.4	Xanthan with high pyruvate, produced with KOH instead of NaOH
13	5.3	5.8	0.3	3.4	Xanthan with high pyruvate, produced with KOH instead of NaOH

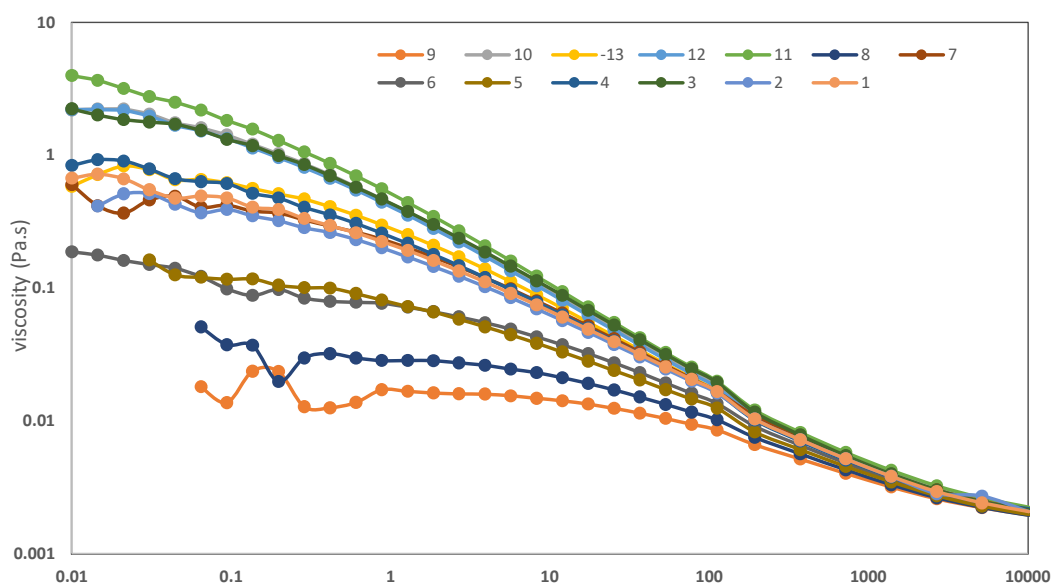


Figure 2. Flow curves of different xanthan types at 30 °C dissolved in 4% NaCl solution.

3.2. Filterability of Xanthan

Filtration tests were conducted using xanthan dissolved in distilled water and brine solutions with varying salinities, as detailed in Table 1. The objective was to assess the impact of salt concentration on xanthan's filterability. A filtration ratio of less than 1.5 was considered acceptable to align with industry standards [22]. Concerns about the standard filtration test have been raised, highlighting that the volume passing through the filter in this test ($\sim 30 \text{ mL/cm}^2$) is significantly lower than in real-world applications, where throughputs can exceed a million ml/cm^2 [33]. Therefore, it is crucial to utilize clarified xanthan to prevent the accumulation of bacterial cells and cell debris, which may be present in conventional xanthan grades and could potentially cause plugging, depending on the pore size and permeability of the reservoir formations [34]. However, comparing the filter test and injectivity in sandstone cores found no differences in test quality. Figure 3 illustrates a clear relationship between the required energy input for achieving the desired filtration ratio and salt concentration. Specifically, the electrical energy needed to dissolve 1 g/L of xanthan at 30 °C increases by 3.3 kWh/m^3 for every additional 1% of total dissolved solids. Dissolution at 30 °C demands more energy than dissolution at 60 °C or filtration of cell-free fermentation broth after diluting to 1 g/L xanthan. Notably, the energy difference between fermentation broth and xanthan powder, dissolved at 30 °C, remains constant in brine solutions. This discrepancy in energy requirements may be attributed to the energy needed to hydrate the powder. In contrast, the energy required to homogenize the fermentation broth to achieve the desired filtration ratio likely stems from other factors.

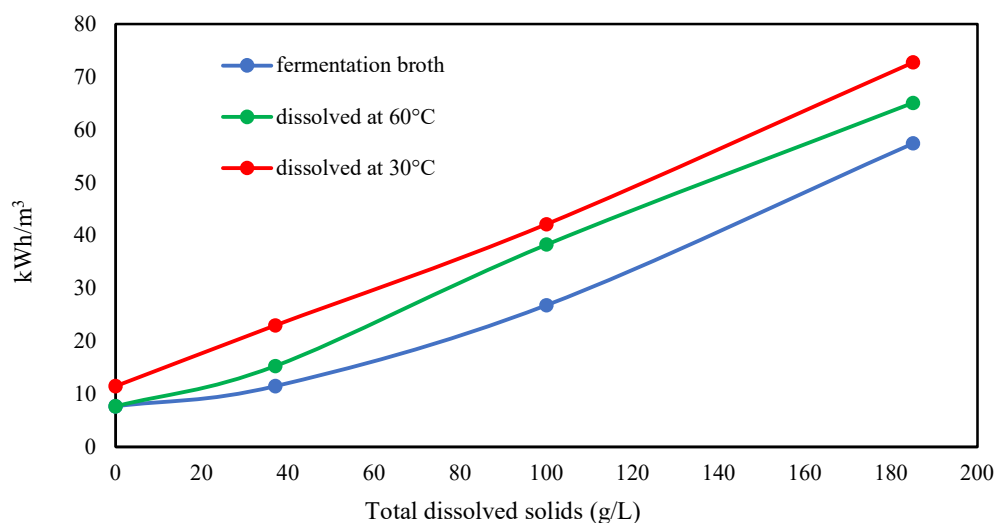


Figure 3. Effect of salt concentration on the electrical energy required to achieve filtration ratio < 1.5 for 1 g/L xanthan dissolution.

It is widely acknowledged that xanthan undergoes a conformational transition from a random coil structure in deionized water to an ordered configuration in the presence of salt [35,36]. The pronounced influence of salt concentrations on the hydration rate of xanthan is argued to be linked to this structural transition [37]. An ordered conformation exhibits a reduced propensity for solubilization due to the lesser entropy gain during dissolution, given the increased rigidity of the molecule. The filtration outcomes in distilled water suggest that the flexible random coils of xanthan molecules pass through the filter more readily than their rigid counterparts.

Xanthan of the strain used for TNCS-ST production was identified as single-stranded through atomic force microscopy analysis [38], displaying greater flexibility than its double-stranded counterpart. It has been proposed that the hydrodynamic radius of xanthan molecules increases with increasing ionic strength [39]. This increase is believed to result from electrostatic repulsion by excess salt ions, prompting the self-association of xan-

than chains. Such association fosters favorable enthalpy interactions, including hydrogen bonding and hydrophobic forces, ultimately forming xanthan chain aggregates.

The dissolution of xanthan was found to create microgels, leading to increased filter and sandstone core plugging [40]. Suggestions were made to replace powdered xanthan with fermentation broth for polymer flooding. However, it is important to note that xanthan powder was dissolved using a Hamilton Beach mixer, which generates low shear forces. The formation of higher multi-chain clusters by associating xanthan molecules is a well-known phenomenon [41]. Filter plugging occurs due to the heterogeneous distribution of polymer network aggregates. Interestingly, these aggregates seem to become more rigid with increasing salt concentration, correlating with the energy required to disentangle the aggregates within the microgels and homogenize the xanthan molecules in the solution. Figure 4 illustrates that an additional 7.7 kWh is needed for every extra 100 g of xanthan per m^3 of formation brine to achieve the desired filtration ratio.

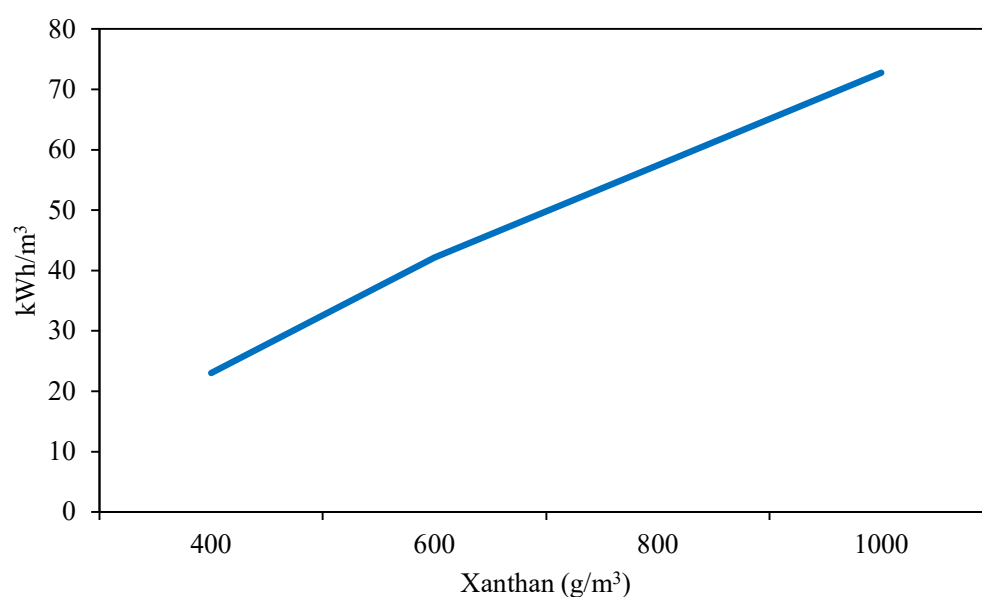


Figure 4. Effect of different xanthan concentration on electrical energy requirements for filtration ratio <1.5 in formation brine at $30\text{ }^{\circ}\text{C}$.

The authors acknowledge that the energy values depicted in Figures 4 and 5 may be specific to the laboratory mixer employed and may differ based on other mixing equipment's size, geometry, and shearing characteristics. Notably, in-line high-shear mixers, frequently employed in various production processes, exhibit greater energy efficiency than laboratory devices. Nevertheless, it is essential to emphasize that the linear relationship between salt concentration, xanthan concentration, and energy input remains consistent and can be extrapolated to production-scale settings.

3.3. Viscosity and Temperature Dependency of Xanthan

Xanthan solutions with a filtration ratio of less than 1.5 underwent subsequent characterization via shear rate-controlled rotational tests. Figure 5 illustrates the flow curves of these diverse solutions, exhibiting the characteristic shear-thinning behavior commonly associated with xanthan. Notably, the viscosity of xanthan demonstrates insensitivity to variations in ionic strength but exhibits slightly lower viscosity in distilled water, particularly in the low-shear region. In contrast to these findings, previous research reported increased intrinsic viscosity for single-stranded xanthan as salinity decreased [36]. Similarly, other studies noted a higher viscosity of xanthan in distilled water than in salt solutions and observed that xanthan viscosity remained relatively insensitive to NaCl concentrations up to 20% [42]. Investigations conducted in our laboratory revealed significant variations

in xanthan viscosity in distilled water, depending on the dissolution method, including shear forces, mixing time, and temperature.

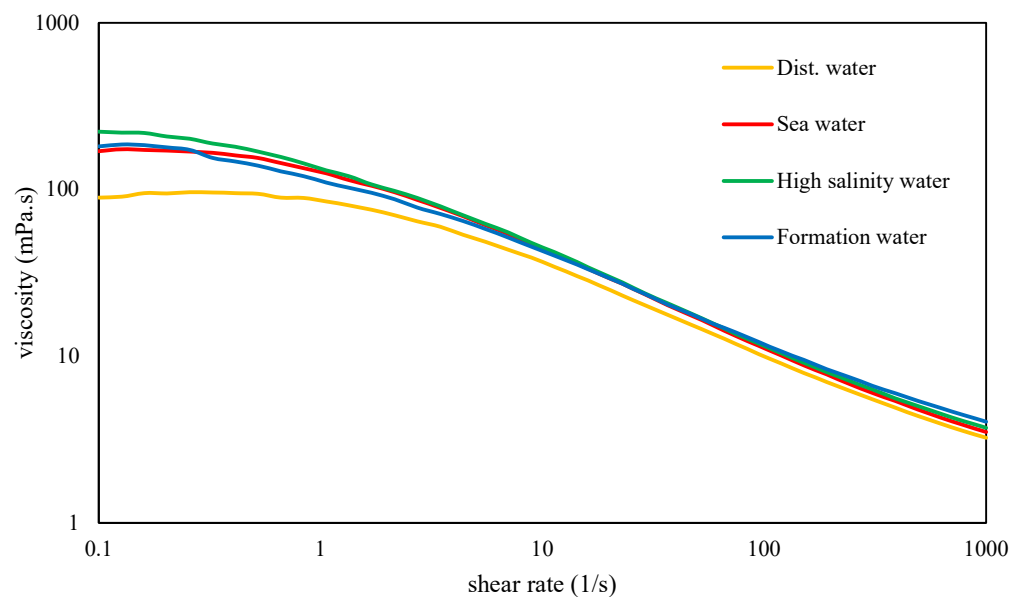


Figure 5. Flow curves of xanthan dissolved in distilled water and various brines at 30 °C with a filtration ratio <1.5.

Figure 6 illustrates the differences in viscosity behavior among various xanthan concentrations in formation brine. It is crucial for a polymer solution used in polymer flooding to exhibit Newtonian behavior in the low-shear region. The higher the zero-shear viscosity of a polymer solution, the greater the force required to surpass the yield point and initiate flow. In instances where well injection is halted due to unforeseen circumstances, excessive pressure could potentially lead to reservoir fracturing and uncontrolled flow behavior.

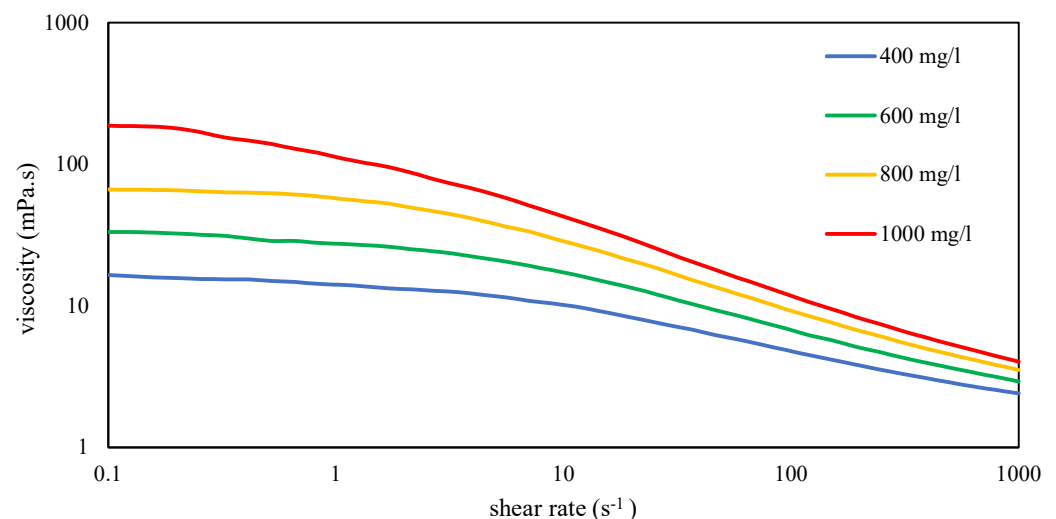


Figure 6. Flow curves of various xanthan concentrations dissolved in high-salinity brine at 30 °C with filtration ratio <1.5.

The viscosity of xanthan exhibits a significant temperature dependency, as illustrated in Figure 7, with viscosity loss gradually escalating as the temperature increases.

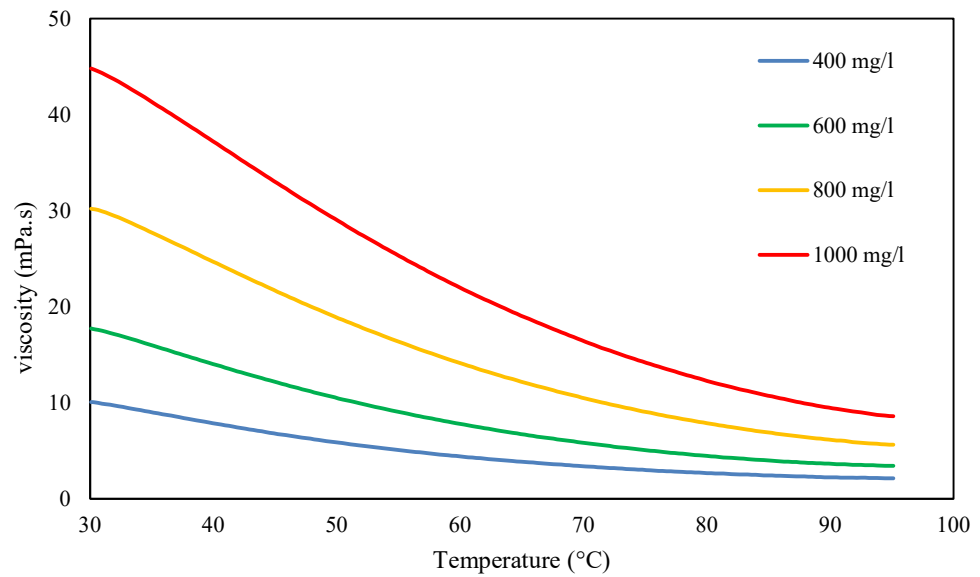


Figure 7. Temperature dependency of various xanthan concentrations dissolved in formation brine at 30 °C with filtration ratio <1.5. Measurements were conducted at a shear rate of 8 s^{-1} .

Xanthan exhibits slightly distinct behavior in distilled water compared to brine solutions. The curves in brines display a sigmoidal shape consistent across varying salt concentrations (Figure 8). A study on the applicability of xanthan in enhanced oil recovery revealed a similar reduction in viscosity with increasing temperatures at a shear rate of 10.8 s^{-1} [43]. It was also noted that viscosity losses increased with decreasing shear rates. This decrease in viscosity was attributed to a conformational transition, shifting from a rod-like, ordered structure to a more flexible, disordered configuration, which was found to be reversible [44].

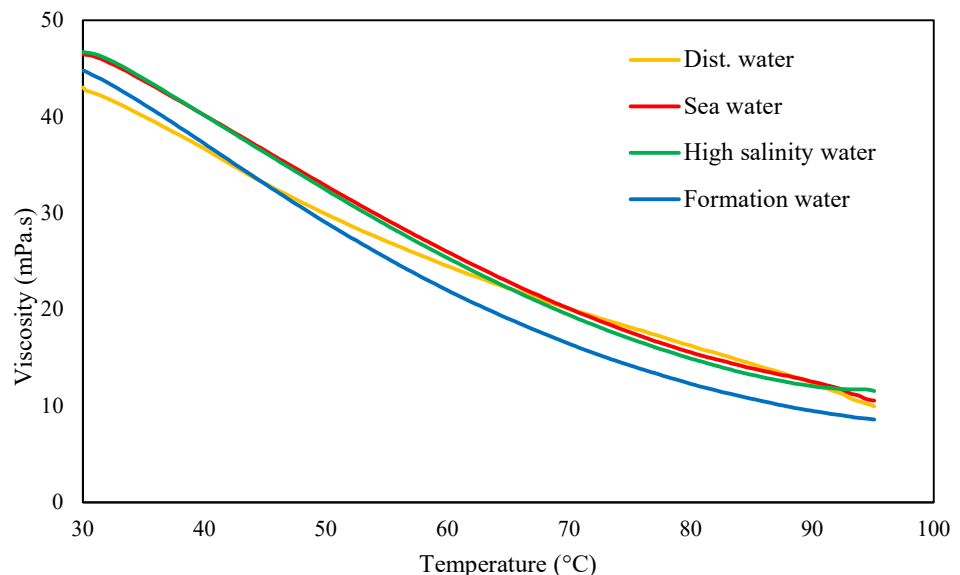


Figure 8. Temperature dependency of 1 g/L xanthan dissolved in distilled water and various brines at 30 °C with filtration ratio <1.5. Measurements were conducted at a shear rate of 8 s^{-1} .

3.4. Shear Stability of Xanthan

Xanthan was dissolved in seawater using a mixing speed of 8000 rpm. The mixing process was halted at specified intervals, and the solution's flow curve was measured. To prevent overheating from energy input, the containers were placed in a water bath at 27 °C

during mixing. The flow curves depicted in Figure 9 reveal a decline in viscosity below a shear rate of $1/s$, while viscosities in the higher shear regions, especially those relevant to enhanced oil recovery, remained unaffected by the duration of mixing.

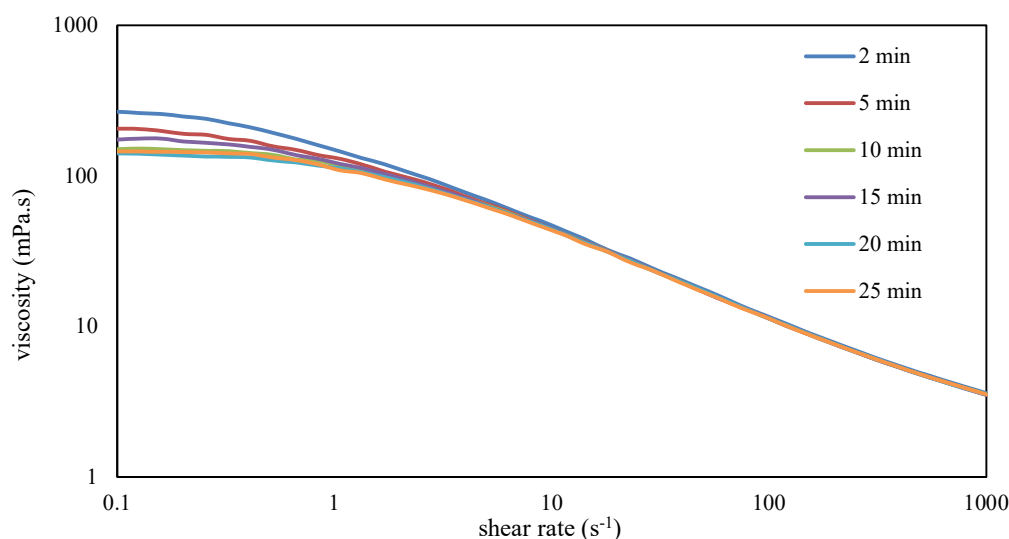


Figure 9. Influence of different mixing durations on the flow curves of 1 g/L xanthan in seawater at a constant shear rate of $42,935 s^{-1}$ at $30\text{ }^{\circ}C$.

A study documented a reduction in molecular weight and gyration radius following high-pressure homogenization treatment applied to xanthan [44]. In another study, where xanthan was compared to various polyacrylamides under conditions more closely resembling those in the field, it was observed that xanthan remained stable even at shear rates as high as $870,000 s^{-1}$, displaying the lowest degree of degradation among all the tested polymers [13].

Additionally, it is worth noting that xanthan reached its maximum viscosity within just 2 min (Figure 9), whereas achieving the acceptable filtration ratio in the same brine took 6 min. This observation underscores that xanthan dissolves rapidly, but high shear forces must subsequently disentangle its network structure to pass through the filter.

3.5. Core Flooding Results

Core flooding experiments were conducted on sandstone and carbonate rock samples under ambient-temperature and high-overburden-pressure conditions to evaluate the effectiveness of polymers in EOR projects. Initially, the cores were saturated with a brine containing 6% NaCl. Oil injection continued until no further expulsion of brine occurred, establishing irreducible water saturation. Subsequently, brine was introduced to simulate secondary oil recovery, followed by three pore volumes of a polymer solution in the tertiary oil recovery phase. The composition of the two tested brines was 1% and 6% NaCl. The results of these experiments are depicted in Figures 10–13, with a comprehensive summary of the runs provided in Table 4.

Xanthan polymer significantly increased oil recovery for the sandstone and carbonate rock. Significantly, it demonstrated improved performance in carbonate rock, leading to remarkable 38% and 67% increases in recovery for both salinity levels, respectively. This difference may be attributed to rock properties, porosity, permeability, and wettability variations between sandstone and carbonate reservoirs. Additionally, the effectiveness of xanthan polymer in altering fluid mobility and enhancing sweep efficiency may vary depending on the specific characteristics of the reservoir rock [3].

Based on the current understanding, future research endeavors should prioritize several key areas in preparing modified xanthan gum for EOR applications. Firstly, there is a need to refine the chemical process of modifying xanthan gum, focusing on optimizing the

rheological properties and EOR potential of the resulting modified polymer. Additionally, post-modification techniques could offer valuable insights into enhancing the compatibility and performance of modified xanthan gum in challenging reservoir environments. These efforts will contribute to advancing the effectiveness and applicability of modified xanthan gum as a viable solution for EOR initiatives.

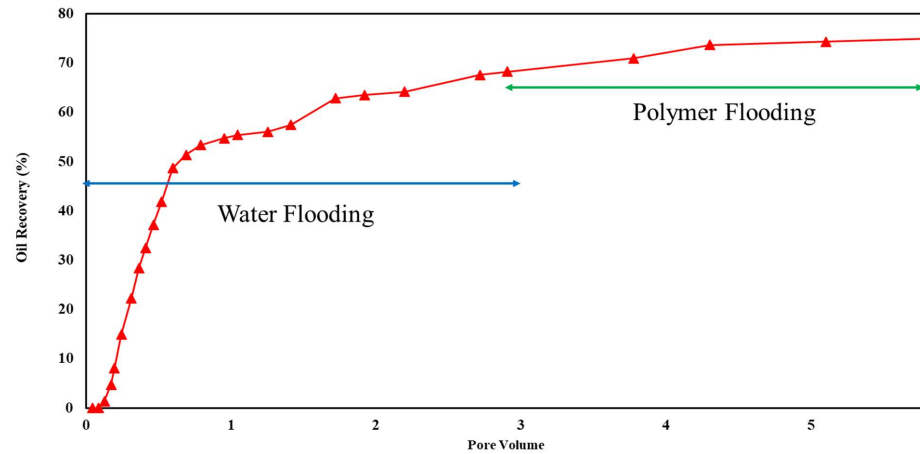


Figure 10. Flooding results of 1500 ppm xanthan concentration in 1% NaCl solution for sandstone rock.

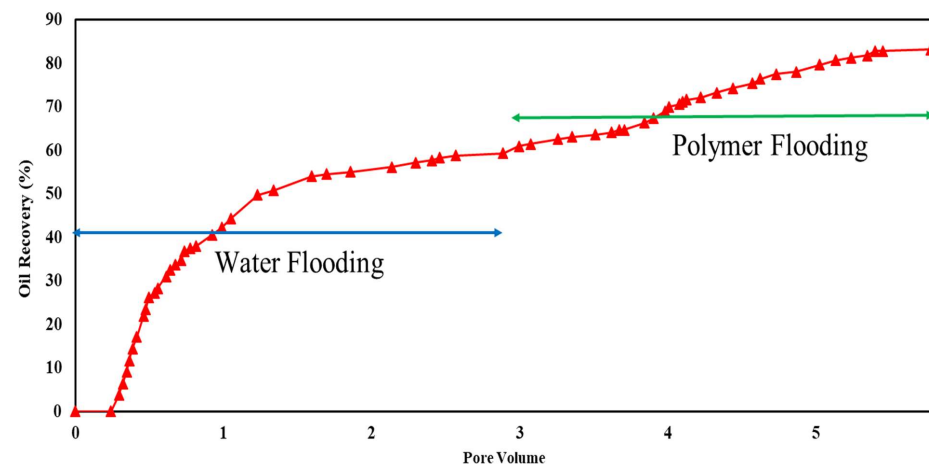


Figure 11. Flooding results of 1500 ppm xanthan concentration in 1% NaCl solution for carbonate rock.

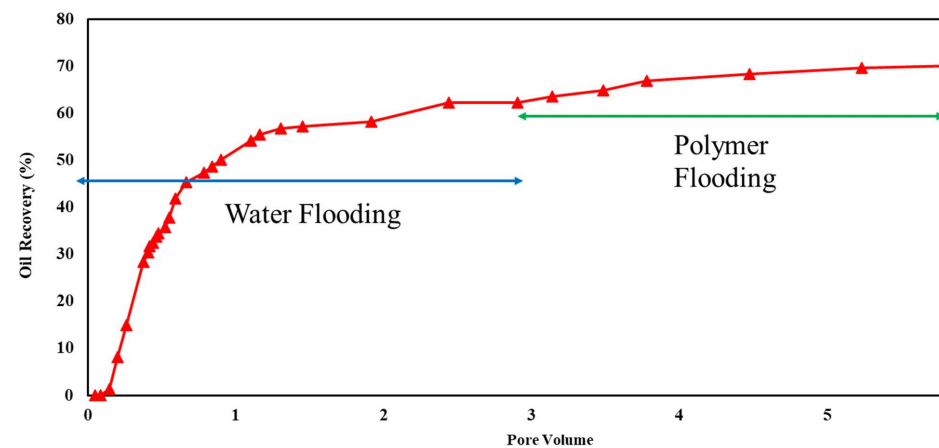


Figure 12. Flooding results of 1500 ppm xanthan concentration in 6% NaCl solution for sandstone rock.

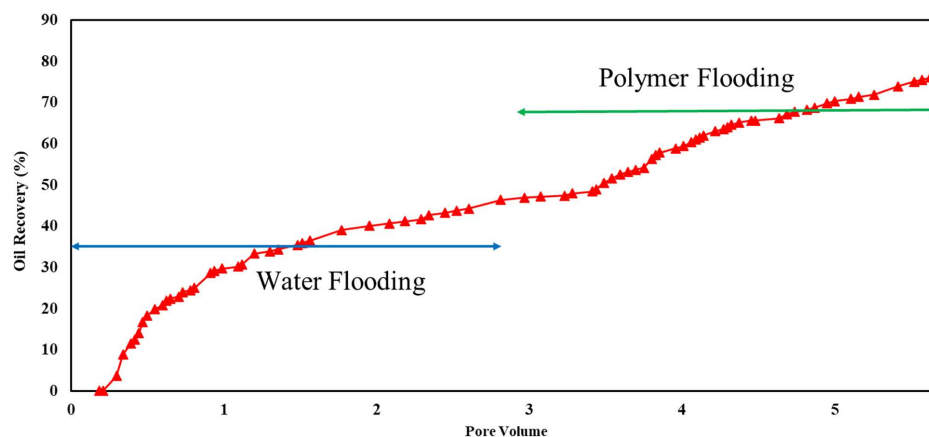


Figure 13. Flooding results of 1500 ppm xanthan concentration in 6% NaCl solution for carbonate rock.

Table 4. Core flooding results of water and polymer floods.

Rock Type	Salinity	Water Flooding Recovery [%]	Polymer Flooding Recovery [%]	Incremental Recovery by Polymer [%]
Sandstone	1 % NaCl	68	75	10
Sandstone	6 % NaCl	62	70	13
Carbonate	1 % NaCl	60	83	38
Carbonate	6 % NaCl	46	77	67

4. Conclusions

In conclusion, this study comprehensively analyzed xanthan TNCS-ST, a specialized polymer tailored for enhanced oil recovery applications. The research highlights the polymer's remarkable transparency and ability to dissolve in high salt concentrations, up to 18% total dissolved solids, making it a promising candidate for EOR operations. The distinctive characteristics of the polymer were thoroughly examined through rigorous laboratory methods, including transparency assessment, salt tolerance testing, and rheological property measurements.

Significantly, the study unveiled a noteworthy correlation between energy input for polymer dissolution and optimal filtration ratios across various brines, presenting a significant advancement in the field. Moreover, insights into the temperature-dependent viscosity behavior of xanthan solutions and observations of uniform flow characteristics within a range of salt content offer valuable understanding for EOR applications.

Moreover, significant oil recovery improvements were noted in sandstone and carbonate rock formations when employing xanthan polymer, with a particularly notable 67% increase in incremental recovery observed in carbonate rock scenarios under high-salinity conditions. These findings underscore the promising potential of xanthan TNCS-ST in improving enhanced oil recovery practices.

Researchers must acknowledge the nuanced nature of xanthan polymers, as their effectiveness may vary due to differences in manufacturing processes. Thus, thoroughly evaluating various xanthan materials is essential to optimize their application in enhanced oil recovery. This study contributes significantly to the body of knowledge in the field and lays a solid foundation for further advancements in EOR technology.

Author Contributions: G.H.: conceptualization, data curation, investigation, methodology development, supervision, writing—original draft; R.K.: investigation, methodology development, formal analysis, data curation, writing—review and editing; A.M.D.: formal investigation, analysis, valida-

tion. H.O.: supervision, methodology development, review and editing. All authors have read and agreed to the published version of the manuscript.

Funding: This research received no external funding.

Data Availability Statement: Data are contained within the article.

Acknowledgments: The authors would like to acknowledge the support provided by the Jungbunzlauer Austria AG.

Conflicts of Interest: Author Gerd Hublik is employed by Jungbunzlauer Austria AG. The remaining authors declare that the research was conducted in the absence of any commercial or financial relationships that could be construed as a potential conflict of interest.

References

- Ghoulmoussi-Barr, S.; Aliouche, D. A Rheological Study of Xanthan Polymer for Enhanced Oil Recovery. *J. Macromol. Sci. Part B Phys.* **2016**, *55*, 793–809. [CrossRef]
- Muhammed, N.S.; Haq, M.B.; Ai-Shehri, D.; Rahman, M.M.; Keshavarz, A.; Hossain, S.M.Z. Comparative Study of Green and Synthetic Polymers for Enhanced Oil Recovery. *Polymers* **2020**, *12*, 2429. [CrossRef]
- Ogunkunle, T.F.; Oni, B.A.; Afolabi, R.O.; Fadairo, A.S.; Ojo, T.; Adesina, O. Comparative analysis of the performance of hydrophobically associating polymers, Xanthan, and guar gum as mobility controlling agents in enhanced oil recovery application. *J. King Saud Univ.—Eng. Sci.* **2022**, *34*, 402–407. [CrossRef]
- Gbadamosi, A.; Shirish Patil, S.; Kamal, M.S.; Adewunmi, A.A.; Yusuff, A.S.; Agi, A.; Oseh, J. Application of Polymers for Chemical Enhanced Oil Recovery: A Review. *Polymers* **2022**, *14*, 1433. [CrossRef] [PubMed]
- Xia, S.; Zhang, L.; Davletsin, A.; Li, Z.; You, J.; Tan, S. Application of polysaccharide biopolymer in petroleum recovery. *Polymers* **2020**, *12*, 1860. [CrossRef] [PubMed]
- American Petroleum Institute. Filterability testing of polymer solutions. In *Recommended Practices for Evaluation of Polymers Used in Enhanced Oil Recovery Operations*, 1st ed.; API Recommended Practice: Washington, DC, USA, 1990; Volume 63.
- Yadali, J.; Kharrat, R. Fundamental Study of Pore Morphology Effect in Low Tension Polymer Flooding or Polymer-Assisted Dilute Surfactant Flooding. *Transp. Porous Media* **2009**, *76*, 199–218. [CrossRef]
- Emami, H.; Kharrat, R.; Wang, X. Study of Microscopic and Macroscopic Displacement Behaviors of Polymer Solution in Water-Wet and Oil-Wet Media. *J. Transp. Porous Media* **2011**, *89*, 97–120. [CrossRef]
- Standnes, D.C.; Skjevraak, I. Literature review of implemented polymer field projects. *J. Pet. Sci. Eng.* **2014**, *122*, 761–775. [CrossRef]
- Lake, L.W.; Johns, R.T.; Rossen, W.R.; Pope, G.A. Polymer methods. In *Fundamentals of Enhanced Oil Recovery*; Society of Petroleum Engineers: Richardson, TX, USA, 2014; Chapter 8; ISBN 978-1-61399-328-6.
- Veiga de Moura, M.R.; Moren, R.Z.L. Concentration, Brine Salinity and Temperature effects on Xanthan Gum Solutions Rheology. *Appl. Rheol.* **2019**, *29*, 69–79. [CrossRef]
- Levitt, D.; Pope, G.A. Selection and screening of polymers for enhanced oil recovery. In *Proceedings of the SPE Symposium on Improved Oil Recovery*, Tulsa, OK, USA, 19–23 April 2008. [CrossRef]
- Zaitoun, A.; Makakou, P.; Blin, N.; Al-Maamari, R.S.; Al-Hashmi, A.R.; Abdel-Goad, M.; Al-Sharji, H.H. Shear Stability of EOR Polymers. *SPE J.* **2012**, *17*, 335–339. [CrossRef]
- Oil & Gas Authority. Polymer Enhanced Oil Recovery—Industry Lessons Learned. 2017. Available online: <https://www.ogauthority.co.uk/news-publications/publications/2017/polymer-enhanced-oil-recovery-industry-lessons-learned/> (accessed on 30 September 2021).
- Wennberg, A.C.; Petersen, K.; Grung, M. *Biodegradation of Selected Offshore Chemicals*; NIVA Report 7218-2017; Norwegian Environment Agency: Oslo, Norway, 2017; ISBN 978-82-577-6953-6.
- Guo, X.H.; Li, W.D.; Tian, J.; Liu, Y.Z. Pilot test of xanthan gum flooding in Shengli oilfield. In *Proceedings of the SPE Asia Pacific Improved Oil Recovery Conference*, Kuala Lumpur, Malaysia, 25–26 October 1999. [CrossRef]
- Seright, R.S.; Wang, D. Polymer flooding: Current status and future directions. *Pet. Sci.* **2023**, *20*, 910–921. [CrossRef]
- Jouenne, S. Polymer flooding in high temperature, high salinity conditions: Selection of polymer type and polymer chemistry, thermal stability. *J. Pet. Sci. Eng.* **2020**, *195*, 107545. [CrossRef]
- Coolman, T.; Alexander, D.; Maharaj, R.; Soroush, M. An evaluation of the enhanced oil recovery potential of the xanthan gum and hydrogel in a heavy oil reservoir in Trinidad. *J. Petrol. Explor. Prod. Technol.* **2020**, *10*, 3779–3789. [CrossRef]
- Saleh, L.D.; Wei, M.; Zhang, Y.; Bai, B. Data analysis for polymer flooding that is based on a comprehensive database. *SPE Reserv. Eval. Eng.* **2017**, *20*, 876–893. [CrossRef]
- Urkedal, H.; Selle, O.M.; Seime, O.J.; Brandal, Ø.; Grøstad, T.; Todosijevic, A.; Dillen, M.; Prasad, D.; Ernst, B.; Lehr, F.; et al. Qualification of Biopolymer in Offshore Single Well Test. In *Proceedings of the Offshore Technology Conference*, Rio de Janeiro, Brazil, 24–26 October 2017. [CrossRef]
- Selle, E.M.; Fischer, H.; Standnes, D.C.; Auflem, I.H.; Lambertsen, A.M.; Mebratu, A.; Gundersen, E.B.; Melien, I. Offshore polymer/lps injectivity test with focus on operational feasibility and near wellbore response in a Heidrun injector. In *Proceedings of the SPE Annual Technical Conference and Exhibition*, New Orleans, LA, USA, 30 September–2 October 2013. [CrossRef]

23. Seright, R.S.; Henrici, B.J. Xanthan stability at elevated temperatures. *SPE Reserv. Eng.* **1990**, *5*, 52–60. [[CrossRef](#)]
24. Kierulf, C.; Sutherland, I.W. Thermal stability of xanthan preparations. *Carbohydr. Polym.* **1988**, *9*, 185–194. [[CrossRef](#)]
25. Lund, T.; Lecourtier, J.; Müller, G. Properties of xanthan solutions after long-term heat treatment at 90 °C. *Polym. Degrad. Stab.* **1990**, *27*, 211–225. [[CrossRef](#)]
26. Littmann, W.; Kleinitz, W.; Christensen, B.E.; Stokke, B.T.; Haugvallstad, T. Late results of a polymer pilot test: Performance, simulation adsorption, and xanthan stability in the reservoir. In Proceedings of the SPE Enhanced Oil Recovery Symposium, Tulsa, OK, USA, 22–24 April 1992. [[CrossRef](#)]
27. Reinoso, D.; Martin-Alfonso, M.J.; Luckham, P.F.; Martinez-Boza, F.J. Rheological characterization of xanthan gum in brine solutions at high temperature. *Carbohydr. Polym.* **2019**, *203*, 103–109. [[CrossRef](#)] [[PubMed](#)]
28. Scott, A.J.; Romero-Zeron, L.; Penlidis, A. Evaluation of polymeric materials for chemical-enhanced oil recovery. *Processes* **2020**, *8*, 361. [[CrossRef](#)]
29. Said, M.; Hag, B.; Al Shehri, D.; Rhman, M.M.; Muhammed, N.S.; Mahmoud, M. Modification of Xanthan Gum for a High-Temperature and High-Salinity Reservoir. *Polym. Polym.* **2021**, *13*, 4212. [[CrossRef](#)]
30. Hublik, G. Xanthan. In *Reference Module in Materials Science and Materials Engineering*; Hashmi, S., Ed.; Elsevier: Oxford, UK, 2016; pp. 1–9.
31. Nsengiyumva, E.M.; Heitz, M.; Alexandrids, P. Salt and Temperature Effects on Xanthan Gum Polysaccharide in Aqueous Solutions. *Int. J. Mol. Sci.* **2024**, *25*, 490. [[CrossRef](#)]
32. Leonhardt, B.; Ernst, B.; Reimann, S.; Steigerwald, A.; Lehr, F. Field testing the polysaccharide schizophyllan: Results of the first year. In Proceedings of the SPE Improved Oil Recovery Symposium, Tulsa, OK, USA, 14–18 April 2014. [[CrossRef](#)]
33. Chauveteau, G.; Kohler, N. Influence of microgels in polysaccharide solutions on their flow behavior through porous media. *SPE J.* **1984**, *24*, 361–368. [[CrossRef](#)]
34. Seright, R.S.; Scheult, J.M.; Talashek, T. Injectivity characteristics of EOR polymers. *SPE Reserv. Eval. Eng.* **2009**, *12*, 783–792. [[CrossRef](#)]
35. Kennedy, J.F.; Bradshaw, I.J. Production, properties, and application of Xanthan. In *Progress of Industrial Microbiology*; Bushell, M.E., Ed.; Elsevier: Amsterdam, The Netherlands, 1984; pp. 319–371.
36. Muller, G.; Aurhourrache, M.; Lecourtier, J.; Chauveteau, G. Salt dependence of the conformation of a single-stranded xanthan. *Int. J. Biol. Macromol.* **1986**, *8*, 167–172. [[CrossRef](#)]
37. To, K.-M.; Mitchell, J.R.; Hill, S.E.; Bardon, L.A.; Matthews, P. Measurement of hydration of polysaccharides. *Food Hydrocoll.* **1994**, *8*, 243–249. [[CrossRef](#)]
38. Teckentrup, J.; Al-Hammood, O.; Steffens, T.; Bednarz, H.; Walhorn, V.; Niehaus, K.; Anselmetti, D. Comparative analysis of different xanthan samples by atomic force microscopy. *J. Biotechnol.* **2017**, *257*, 2–8. [[CrossRef](#)] [[PubMed](#)]
39. Southwick, J.G.; Jamieson, A.M.; Blackwell, J. Conformation of Xanthan dissolved in aqueous urea and sodium chloride solutions. *Carbohydr. Res.* **1982**, *99*, 117–127. [[CrossRef](#)]
40. Kohler, N.; Chauveteau, G. Xanthan polysaccharide plugging behavior in porous media—Preferential use of fermentation broth. *J. Pet. Technol.* **1981**, *33*, 349–358. [[CrossRef](#)]
41. Stokke, B.T.; Christensen, B.E.; Smidsrod, O. Macromolecular properties of Xanthan. In *Polysaccharides: Structural Diversity and Functional Versatility*; Dumitriu, S., Ed.; Marcel Dekker: New York, NY, USA, 1998; pp. 433–472.
42. Jang, H.Y.; Zhang, K.; Chon, B.H.; Choi, H.J. Enhanced oil recovery performance and viscosity characteristics of polysaccharide Xanthan gum solution. *J. Ind. Eng. Chem.* **2015**, *21*, 741–745. [[CrossRef](#)]
43. Milas, M.; Rinaudo, M. Conformational investigation on the bacterial polysaccharide xanthan. *Carbohydr. Res.* **1979**, *76*, 189–196. [[CrossRef](#)]
44. Gulrez, S.K.H.; Al-Assaf, S.; Fang, Y.; Phillips, G.O.; Gunning, A.P. Revisiting the conformation of Xanthan and the effect of industrially relevant treatments. *Carbohydr. Polym.* **2012**, *90*, 1235–1243. [[CrossRef](#)]

Disclaimer/Publisher’s Note: The statements, opinions and data contained in all publications are solely those of the individual author(s) and contributor(s) and not of MDPI and/or the editor(s). MDPI and/or the editor(s) disclaim responsibility for any injury to people or property resulting from any ideas, methods, instructions or products referred to in the content.